Inorg. Chem. **2003**, *42*, 7658–7665

Heterotrimetallic 4f–3d Coordination Polymers: Synthesis, Crystal Structure, and Magnetic Properties

Hui-Zhong Kou,* Bei Chuan Zhou, and Ru-Ji Wang

Department of Chemistry, Tsinghua University, Beijing 100084, P. R. China

Received July 18, 2003

A series of cyano-bridged heterotrimetallic complexes $[CuL]_2Ln(H_2O)_2M(CN)_6 \cdot 7H_2O$ have been synthesized by the reactions of CuL (L^{2-} = dianion of 1,4,8,11-tetraazacyclotradecane-2,3-dione), Ln^{3+} (Ln = Gd or La), and $[M(CN)_6]^{3-}$ (M = Co, Fe, or Cr). X-ray diffraction analysis reveals that these complexes are isostructural and have a novel chain structure. The Ln^{3+} ion is eight-coordinated by six oxygen atoms of two CuL and two water molecules and two nitrogen atoms of the bridging cyano ligands of two $[M(CN)_6]^{3-}$, while the $[M(CN)_6]^{3-}$ anion connects two Ln^{3+} using two trans-CN^- ligands giving rise to a chainlike structure. In the chain, every CuL group tilts toward the CN^- ligand of adjacent $[M(CN)_6]^{3-}$ with the Cu–N_{cyano} contacts ranging from 2.864(6) to 2.930(6) Å. Magnetic studies on the CuGdCo complex (**1**) indicate the presence of ferromagnetic coupling between Cu(II) and Gd(III). The CuLaCr (**5**) and CuLaFe (**2**) complexes exhibit ferromagnetic interaction between paramagnetic Cu(II) and Cr(III)/Fe(III) ions through the weak cyano bridges (Cu–N_{cyano} = 2.930(6) Å for **2**). A global ferromagnetic interaction is operative in the CuGdFe complex (**3**) with the concurrence of dominant ferromagnetic Cu(II)–Gd(III) and minor antiferromagnetic Gd(III)–Fe(III) as well as the ferromagnetic Cu(II)–Fe(III) interaction. For the CuGdCr complex (**4**), an overall antiferromagnetic behavior was observed, which is attributed to the presence of dominant antiferromagnetic Cr^{III}–Gd^{III} coupling and the minor ferromagnetic Cu^{II}–Gd^{III} and Cu^{II}–Cr^{III} interaction. Moreover, a spin frustration phenomenon was found in complex **4**, which results from the ferro–ferro–antiferromagnetic exchanges in the trigonal Cu–Gd–Cr units. The magnetic susceptibilities of these complexes were simulated using suitable models. The magneto–structural correlation was investigated. These complexes did not show a magnetic phase transition down to 1.8 K.

Introduction

The construction of extended or isolated compounds with a particular structure and tunable physical properties is of current interest.[1] Magnetism of such compounds is an active field of research, involving chemistry, physics, biology, and material science.[2] Until now, the mechanism of magnetic coupling between 3d metal ions has been well understood; however, that between 3d and 4f metal ions is complicated, and little has been known.[3−27] Much attention has been paid to the investigation of the magnetic interaction between a 3d and the isotropic Gd^{3+} ion since the situation is easy to

* To whom correspondence should be addressed. E-mail: kouhz@mail.tsinghua.edu.cn. Fax: 86-10-62788765.

(1) Yaghi, O. M.; O'Keeffe, M.; Kanatzidis, M. *J. Solid State Chem.* **2000**, *152*, 1. Liu, J. P.; Knoeppel, D. W.; Liu, S. M.; Meyers, E. A.; Shore, S. G. *Inorg. Chem.* **2001**, *40*, 2842. Knoeppel, D. W.; Shore, S. G. *Inorg. Chem.* **1996**, *35*, 5328. Knoeppel, D. W.; Liu, J.; Meyers, E. A.; Shore, S. G. *Inorg. Chem.* **1998**, *37*, 4828.
(2) Kahn, O. *Molecular Magnetism*; VCH: Weinheim, Germany, 1993.
(3) Tang, J.-K.; Li, Y.-Z.; Wang, Q.-L.; Gao, E.-Q.; Liao, D.-Z.; Jiang, Z.-H.; Yan, S.-P.; Cheng, P.; Wang, L.-F.; Wang, G.-L. *Inorg. Chem.* **2002**, *41*, I2188.
(4) Zhao, B.; Cheng, P.; Dai, Y.; Cheng, C.; Liao, D.-Z.; Yan, S.-P.; Jiang, Z.-H.; Wang, G.-L. *Angew. Chem., Int. Ed.* **2003**, *42*, 934.
(5) Baggio, R.; Garland, M. T.; Moreno, Y.; Pena, O.; Perec, M.; Spodine, E. *J. Chem. Soc., Dalton Trans.* **2000**, 2061.
(6) Rizzi, A. C.; Calvo, R.; Baggio, R.; Garland, M. T.; Pena, O.; Perec, M. *Inorg. Chem.* **2002**, *41*, 5609.
(7) Yan, B.; Chen, Z. *Helv. Chim. Acta* **2001**, *84*, 817. Yan, B.; Chen, Z. D.; Wang, S. X. *Transition Met. Chem.* **2001**, *26*, 287.
(8) Tanase, S.; Andruh, M.; Muller, A.; Schmidtmann, M.; Mathoniere, C.; Rombaut, G. *Chem. Commun.* **2001**, 1084.
(9) Bayly, S. R.; Xu, Z. Q.; Patrick, B. O.; Rettig, S. J.; Pink, M.; Thompson, R. C.; Orvig, C. *Inorg. Chem.* **2003**, *42*, 1576.
(10) Ren, Y. P.; Long, L. S.; Mao, B. W.; Yuan, Y. Z.; Huang, R. B.; Zheng, L. S. *Angew. Chem., Int. Ed.* **2003**, *42*, 532.
(11) Liu, Q.-D.; Li, J.-R.; Gao, S.; Ma, B.-Q.; Kou, H.-Z.; Liang, O.-Y.; Huang, R.-L.; Zhang, X. X.; Yu, K.-B. *Eur. J. Inorg. Chem.* **2003**, 731.
(12) Liu, Q.-D.; Gao, S.; Li, J.-R.; Zhou, Q.-Z.; Yu, K.-B.; Ma, B.-Q.; Zhang, S.-W.; Zhang, X. X.; Jin, T.-Z. *Inorg. Chem.* **2000**, *39*, 2488.
(13) Cui, Y.; Chen, J. T.; Long, D. L.; Zheng, F. K.; Cheng, W. D.; Huang, J. S. *J. Chem. Soc., Dalton Trans.* **1998**, 2955.

10.1021/ic0348502 CCC: $25.00
Published on Web 10/17/2003

deal with. Focusing on the magnetism of widely studied Cu^{2+} and Gd^{3+},[28−49] we can find that both ferromagnetic[28−46] and antiferromagnetic[5,47−49] interactions are observed although the former case is more commonly observed. Therefore, the intrinsic ferromagnetic $Cu^{II}-Gd^{III}$ coupling was doubted.[48] This shows the complexity of Cu(II)−Gd(III) magnetic interaction. This requires more examples to elucidate the mechanism.

The oxamidato-bridged $Gd^{III}-Cu^{II}$ complexes have been investigated magnetically, and the first oxamidato-bridged Ln^{3+}-containing ferromagnet has been reported.[50] Recently, four-coordinate macrocyclic oxamido−Cu^{II} complex CuL (L = dianion of 1,4,8,11-tetraazacyclotradecane-2,3-dione) has been utilized to successfully construct a polynuclear Cu_6Nd_2 complex.[3] The reaction among CuL, Gd^{3+}, and $[Cr(CN)_6]^{3-}$ has resulted in the successful synthesis of a novel mixed ligand-bridged 2D heterotrimetallic coordination polymer $Gd[CuL]_4Cr(CN)_6 \cdot 5H_2O$.[51] This complex contains oxamidato-bridged $Cu^{II}-Gd^{III}$ and cyano-bridged $Cu^{II}-Cr^{III}$ moieties, and no $Cr^{III}-NC-Gd^{III}$ linkages are present in the complex. The weak $Cu^{II}-Cr^{III}$ interaction precludes magnetic ordering in the complex. We sought to design extended species with $Cr^{III}-NC-Gd^{III}$ linkages that might exhibit interesting magnetic behavior and possibly magnetic ordering. A series of such complexes have been synthesized and characterized structurally and magnetically. Herein we present the design, synthesis, crystal structure, and magnetic properties of the compounds.

Experimental Section

Elemental analyses of carbon, hydrogen, and nitrogen were carried out with an Elementar Vario EL. The infrared spectroscopy was performed on a Magna-IR 750 spectrophotometer in the 4000−400 cm^{-1} region. TGA measurement of **2** was performed in the temperature range 30−300 °C under nitrogen on a Universal V2.6D TA instrument. The powder XRD plot of **5** was recorded on a Brucker D8-advance X-ray powder diffractometer with Cu Kα radiation (λ = 1.5406 Å). Variable-temperature magnetic susceptibility measurements were performed on a Quantum Design MPMS SQUID and a MagLab 2000 magnetometer. Zero-field ac magnetic susceptibility and field dependence of magnetization measurements were on a MagLab 2000 magnetometer. The experimental susceptibilities were corrected for the diamagnetism of the constituent atoms (Pascal's tables).

Syntheses. The precursors CuL,[52] $K_3[Co(CN)_6]$,[53] and $K_3[Cr(CN)_6] \cdot H_2O$[54] were prepared by the literature methods.

CuGdCo (1). An aqueous solution of $K_3[Co(CN)_6]$ was carefully layered with an aqueous solution of CuL and $GdCl_3 \cdot 6H_2O$ mixture (molar ratio = 2:1). Block violet single crystals of **1** formed at the interface in 2 weeks. Yield: 10%. IR (KBr, cm^{-1}): ν(C≡N), 2121 s, 2140 vs, ν(C═O), 1616 vs. Anal. Calcd for $C_{26}H_{54}CoCu_2GdN_{14}O_{13}$: C, 28.03; H, 4.89; N, 17.60. Found: C, 28.09; H, 4.76; N, 17.61.

CuLaFe (2), CuGdFe (3), CuGdCr (4), and CuLaCr (5). Complexes **2**−**5** were synthesized using a procedure similar to that for **1**. Block brown single crystals of **2** and **3** and block violet single crystals of **4** and **5** were obtained. IR (KBr, cm^{-1}) for **2**: ν(C≡N),

(14) Costes, J. P.; Dahan, F.; Dupuis, A.; Laurent, J. P. *Chem.—Eur. J.* **1998**, *4*, 1616.
(15) Kido, T.; Ikuta, Y.; Sunatsuki, Y.; Ogawa, Y.; Matsumoto, N. *Inorg. Chem.* **2003**, *42*, 398.
(16) Figuerola, A.; Diaz, C.; Ribas, J.; Tangoulis, V.; Granell, J.; Lloret, F.; Mahia, J.; Maestro, M. *Inorg. Chem.* **2003**, *42*, 641.
(17) Yang, Y. Y.; Chen, X. M.; Ng, S. W. *J. Solid State Chem.* **2001**, *161*, 214.
(18) Liang, Y. C.; Hong, M. C.; Su, W. P.; Cao, R.; Zhang, W. J. *Inorg. Chem.* **2001**, *40*, 4574.
(19) Chen, X. M.; Yang, Y. Y. *Chin. J. Chem.* **2000**, *18*, 664.
(20) Xu, Z. Q.; Read, P. W.; Hibbs, D. E.; Hursthouse, M. B.; Malik, K. M. A.; Patrick, B. O.; Rettig, S. J.; Seid, M.; Summers, D. A.; Pink, M.; Thompson, R. C.; Orvig, C. *Inorg. Chem.* **2000**, *39*, 508.
(21) Legendziewicz, J.; Borzechowska, M. G.; Oczko, G.; Meyer, G. *New J. Chem.* **2000**, *24*, 53.
(22) Azuma, M.; Kaimori, S.; Takano, M. *Chem. Mater.* **1998**, *10*, 3124.
(23) Kou, H.-Z.; Gao, S.; Jin, X. L. *Inorg. Chem.* **2001**, *40*, 6295.
(24) Breeze, S. R.; Wang, S. N.; Greedan, J. E.; Raju, N. P. *J. Chem. Soc., Dalton Trans.* **1998**, 2327.
(25) Decurtins, S.; Gross, M.; Schmalle, H. W.; Ferlay, S. *Inorg. Chem.* **1998**, *37*, 2443.
(26) Chen, X.-M.; Aubin, S. M. J.; Wu, Y.-L.; Yang, Y.-S.; Mak, T. C. W.; Hendrickson, D. N. *J. Am. Chem. Soc.* **1995**, *117*, 9600.
(27) Kahn, M. L.; Mathoniere, C.; Kahn, O. *Inorg. Chem.* **1999**, *38*, 3692.
(28) Bencini, A.; Benelli, C.; Caneschi, A.; Barlin, R. L.; Dei, A.; Gatteschi, D. *J. Am. Chem. Soc.* **1985**, *107*, 8128.
(29) Bencini, A.; Benelli, C.; Caneschi, A.; Dei, A.; Gatteschi, D. *Inorg. Chem.* **1986**, *25*, 572. Costes, J.-P.; Dahan, F.; Dupuis, A. *Inorg. Chem.* **2000**, *39*, 165.
(30) Andruh, M.; Ramade, I.; Codjovi, E.; Guillou, O.; Kahn, O.; Trombe, J. C. *J. Am. Chem. Soc.* **1993**, *115*, 1822.
(31) Zhang, L.; Wang, S. B.; Yang, G. M.; Tang, J. K.; Liao, D. Z.; Jiang, Z. H.; Yan, S. P.; Cheng, P. *Inorg. Chem.* **2003**, *42*, 1462.
(32) Benelli, C.; Blake, A. J.; Milne, P. E. Y.; Rawson, J. M.; Winpenny, R. E. P. *Chem.—Eur. J.* **1995**, *1*, 614.
(33) Costes, J. P.; Dahan, F.; Dupuis, A.; Laurent, J. P. *New J. Chem.* **1998**, *22*, 1525. Costes, J.-P.; Dahan, F.; Dupuis, A.; Laurent, J.-P. *Inorg. Chem.* **1996**, *35*, 2400.
(34) Sakamoto, M.; Kitakami, Y.; Sakiyama, H.; Nishida, Y.; Fukuda, Y.; Sakai, M.; Sadaoka, Y.; Matsumoto, A.; Okawa, H. *Polyhedron* **1997**, *16*, 3345.
(35) Ryazanov, M.; Nikiforov, V.; Lloret, F.; Julve, M.; Kuzmina, N.; Gleizes, A. *Inorg. Chem.* **2002**, 1816.
(36) Shiga, T.; Ohba, M.; Okawa, H. *Inorg. Chem. Commun.* **2003**, *6*, 15.
(37) Ramade, I.; Kahn, O.; Jeannin, Y.; Robert, F. *Inorg. Chem.* **1997**, *36*, 930.
(38) Benelli, C.; Fabretti, A. C.; Giusti, A. *J. Chem. Soc., Dalton Trans.* **1993**, 409. Benelli, C.; Caneschi, A.; Gatteschi, D.; Guillou, O.; Pardi, L. *Inorg. Chem.* **1990**, *29*, 1750.
(39) Sanz, J. L.; Ruiz, R.; Gleizes, A.; Lloret, F.; Faus, J.; Julve, M.; Borras-Almenar, J. J.; Journaux, Y. *Inorg. Chem.* **1996**, *35*, 7384.
(40) Guillou, O.; Bergerat, P.; Kahn, O.; Bakalbassis, E.; Boubekeur, K.; Batail, P.; Guillot, M. *Inorg. Chem.* **1992**, *31*, 110.
(41) Avecilla, F.; Platas-Iglesias, C.; Rodriguez-Cortinas, R.; Guillemot, G.; Bunzli, J. C. G.; Brondino, C. D.; Geraldes, C. F. G. C.; de Blas, A.; Rodriguez-Blas, T. *J. Chem. Soc., Dalton Trans.* **2002**, 4658.
(42) Li, Z.-S.; Sun, H.-L.; Kou, H.-Z.; Han, S.-T.; Gao, S. *J. Rare Earths* **2002**, *20*, 343.
(43) Chen, Q. Y.; Luo, Q. H.; Fu, D. G.; Chen, J. T. *J. Chem. Soc., Dalton Trans.* **2002**, 2873.
(44) Atria, A. M.; Moreno, Y.; Spodine, E.; Garland, M. T.; Baggio, R. *Inorg. Chim. Acta* **2002**, *335*, 1.
(45) Liang, Y.; Cao, R.; Su, W.; Hong, M.; Zhang, W. *Angew. Chem., Int. Ed.* **2000**, *39*, 3304.
(46) Liu, Q.-D.; Gao, S.; Li, J.-R.; Ma, B.-Q.; Zhou, Q.-Z.; Yu, K.-B. *Polyhedron* **2002**, *21*, 1097.
(47) Gao, S.; Borgmeier, O.; Leuken, H. *Acta Phys. Pol., A* **1996**, *90*, 393.
(48) Costes, J.-P.; Dahan, F.; Dupuis, A.; Laurent, J.-P. *Inorg. Chem.* **2000**, *39*, 169. Costes, J.-P.; Dahan, F.; Dupuis, A. *Inorg. Chem.* **2000**, *39*, 5994.
(49) Chen, X.-M.; Wu, Y.-L.; Yang, Y.-Y.; Aubin, S. M. J.; Hendrickson, D. N. *Inorg. Chem.* **1998**, *37*, 6186.
(50) Bartolome, F.; Bartolome, J.; Oushoorn, R. L.; Guillou, O.; Kahn, O. *J. Magn. Magn. Mater.* **1995**, *140*, 1711.
(51) Kou, H.-Z.; Zhou, B. C.; Gao, S.; Wang, R.-J. *Angew. Chem., Int. Ed.* **2003**, *42*, 3288.
(52) Cronin, L.; Mount, A. R.; Parsons, S.; Robertson, N. *J. Chem. Soc., Dalton Trans.* **1999**, 1925.
(53) Bertini, I.; Luchinat, C.; Mani, F.; Scozzafava, A. *Inorg. Chem.* **1980**, *19*, 1333.
(54) Cruser, F. V. D.; Miller, E. H. *J. Am. Chem. Soc.* **1906**, *28*, 1132.

Table 1. Crystal Data for Complexes **1**−**4**

	1	**2**	**3**	**4**
formula	$C_{26}H_{54}CoCu_2GdN_{14}O_{13}$	$C_{26}H_{54}FeCu_2LaN_{14}O_{13}$	$C_{26}H_{54}FeCu_2GdN_{14}O_{13}$	$C_{26}H_{54}CrCu_2GdN_{14}O_{13}$
fw	1114.09	1092.67	1111.01	1107.16
space group	*C*2/*c*	*C*2/*c*	*C*2/*c*	*C*2/*c*
a/Å	27.413(8)	27.746(10)	27.510(9)	28.006(8)
b/Å	10.130(3)	10.096(4)	10.130(3)	10.1441(18)
c/Å	19.067(5)	19.083(7)	19.055(6)	19.041(3)
β/deg	129.810(4)	129.075(5)	129.767(4)	129.622(9)
V/Å^3	4067(2)	4150(3)	4082(2)	4166.8(15)
Z	4	4	4	4
ρ_{calcd}/g cm^{-3}	1.819	1.749	1.808	1.765
μ(Mo Kα)/mm^{-1}	3.118	2.437	3.056	2.906
data/restraint/params	3550/0/260	4269/0/260	4184/0/260	3669/0/260
GOF	1.014	1.018	1.022	1.090
R1 [$I > 2\sigma(I)$]	0.0405	0.0529	0.0392	0.0414
wR2 (all data)	0.0886	0.1110	0.1003	0.1093

2124 s, 2111 s, 2026 sh; ν(O≡N) 1614 vs. Anal. Calcd for $C_{26}H_{54}FeCu_2LaN_{14}O_{13}$: C, 28.58; H, 4.98; N, 17.95. Found: C, 28.67; H, 4.82; N, 18.15. IR (KBr, cm^{-1}) for **3**: ν(C≡N), 2129 s, 2110 s; ν(O═C) 1618 vs. Anal. Calcd for $C_{26}H_{54}FeCu_2GdN_{14}O_{13}$: C, 28.11; H, 4.90; N, 17.65. Found: C, 28.10; H, 4.74; N, 17.70. IR (KBr, cm^{-1}) for **4**: ν(C≡N), 2150 s, 2126 s; ν(O═C) 1617 vs. Anal. Calcd for $C_{26}H_{54}CrCu_2GdN_{14}O_{13}$: C, 28.21; H, 4.92; N, 17.71. Found: C, 27.55; H, 4.95; N, 17.44. IR (KBr, cm^{-1}) for **5**: ν(C≡N), 2146 s, 2127 s; ν(O═C) 1614 vs, 1603 sh. Anal. Calcd for $C_{26}H_{54}CrCu_2LaN_{14}O_{13}$: C, 28.68; H, 5.00; N, 18.01. Found: C, 28.52; H, 4.99; N, 18.05.

X-ray Structure Determination. The data collection of **1**−**3** was made on a Bruker Smart CCD (293 K), and that of **4** on a Simens Bruker P4 diffractometer. Intensity data were corrected for *LP* factors. The absorption corrections have been applied by using SADABS (Bruker 2000) for complexes **1**−**3** and ψ-scan for complex **4**. The structures were solved by direct methods SHELXS-97 and refined by full-matrix least squares (SHELXL-97) on F^2. Hydrogen atoms attached to the C and N atoms were added geometrically and refined using a riding model. The hydrogen atoms attached to oxygen atoms were found from the Fourier map and fixed using AFIX. For complexes **2**−**4**, the high residual peaks and holes are observed in the vicinity of Gd^{3+}, which are normal for complexes containing heavy atoms. The crystal data are summarized in Table 1.

Results and Discussion

Synthesis and General Characterization. Cyano-bridged 4f−3d complexes form a family of magnetic materials.[55−60] We have recently reported a 2D heterotrimetallic Gd-$[CuL]_4Cr(CN)_6\cdot 5H_2O$ prepared by the reaction of $GdCl_3\cdot 6H_2O$, CuL, and $K_3[Cr(CN)_6]$ in a molar ratio of 1:4:1.[51] No bridging Gd−N≡C−Cr linkages are present in the complex. Attempts are being made to synthesize polymeric Gd−Cu−Cr species with the hope of long-range magnetic ordering. Using less amounts of CuL, i.e., CuL:Ln = 2:1, we successfully synthesized a series of one-dimensional chain-like complexes $[CuL]_2Ln(H_2O)_2M(CN)_6]\cdot 7H_2O$. The employment of larger amounts of CuL always led to the 2D species. The complex $[CuL]_2La(H_2O)_2Cr(CN)_6\cdot 7H_2O$ (**5**) does not diffract properly, and therefore, the structure of **5** was determined via powder XRD (see Supporting Information), IR, and microelemental analyses (CHN) measurements. The powder XRD spectrum of **5** resembles that of complexes **2** and **4**, suggesting that complex **5** is analogous to complexes **1**−**4**.

The IR spectra of the complexes are similar and show the splitting of the ν(C≡N) bands in the range 2000−2200 cm^{-1}, suggestive of the presence of both bridged and nonbridged CN^- ligands. The strong band at ca. 1616 cm^{-1} is assigned to the C═O stretching vibration (L).

The TGA of complex **2** shows a weight loss of 11.6% in the temperature range 70−108 °C, corresponding to the interstitial seven water molecules. The additional loss of water molecules (the coordinated water molecules) ensues above 110 °C. Above 200 °C, successive mass loss was observed, suggesting decomposition of the sample (see Supporting Information).

Crystal Structures. Selected bond distances and angles for complexes **1**−**4** are listed in Table 2.

X-ray crystallography reveals that the structures of **1**−**4** are isomorphous. As shown in Figure 1, the structure consists of a neutral chain, which is formed by an alternating $[M(CN)_6]^{3-}$ and $[CuL(H_2O)]_2Ln(H_2O)_2^{3+}$ units. Two trans-cyano ligands of $[M(CN)_6]^{3-}$ are linked to the $[CuL(H_2O)]_2Ln(H_2O)_2^{3+}$ units, with the C≡N−Ln bond angle of 171.0(5)° for **1**, 173.0(4)° for **2**, 172.1(4)° for **3**, and 172.5(5)° for **4**. The Ln(III) ion is eight-coordinated by two cyano nitrogen atoms and six oxygen atoms of two CuL and two water molecules. Two CuL groups lie in the opposite position around Ln^{3+} and tilt a little toward the cyano nitrogen atom (N12) of $M(CN)_6^{3-}$. The long Cu(1)−N(12)$^{\#2}$ bond distances of 2.930(6) for **1**, 2.916(6) for **2**, 2.864(6) for **3**, and 2.868(6) Å for **4** indicate the existence of weak coordination interactions between Cu(1) and the cyano nitrogen atom. The corresponding Cu(1)−N(12)$^{\#2}$−C(12)$^{\#2}$ bond angles range from 122.57(46) to 125.65(46)°. The octahedral coordination sphere of Cu(1) is completed by the water oxygen atom O(3W) with the Cu(1)−O(3W) bond distances of 2.748(6)

(55) Hulliger, F.; Landolt, M.; Vetsch, H. *J. Solid State Chem.* **1976**, *18*, 283.
(56) Ma, B.-Q.; Gao, S.; Su, G.; Xu, G.-X. *Angew. Chem., Int. Ed.* **2001**, *40*, 434.
(57) Gao, S.; Su, G.; Yi, T.; Ma, B.-Q. *Phys. Rev. B* **2001**, *63*, 054432.
(58) Figuerola, A.; Diaz, C.; El Fallah, M. S.; Ribas, J.; Maestro, M.; Mahia, J. E. *Chem. Commun.* **2001**, 1204.
(59) Kou, H.-Z.; Gao, S.; Sun, B.-W.; Zhang, J. *Chem. Mater.* **2001**, *13*, 1431.
(60) Kou, H.-Z.; Gao, S.; Li, C.-H.; Liao, D.-Z.; Zhou, B. C.; Wang, R.-J.; Li. Y.-D. *Inorg. Chem.* **2002**, *41*, 4756.

Table 2. Selected Bond Distances (Å) and Angles (deg)[a]

	1	2	3	4
Ln(1)−O(1)	2.381(4)	2.480(4)	2.383(4)	2.386(4)
Ln(1)−O(2)	2.396(4)	2.498(4)	2.391(4)	2.387(3)
Ln(1)−O(1W)	2.421(4)	2.526(5)	2.426(4)	2.425(4)
Ln(1)−N(11)	2.531(5)	2.629(5)	2.522(4)	2.504(4)
Cu(1)−N(1)	1.989(6)	1.982(6)	1.992(5)	1.987(5)
Cu(1)−N(2)	1.983(6)	1.984(6)	1.989(5)	1.989(5)
Cu(1)−N(3)	1.952(5)	1.947(5)	1.951(5)	1.945(5)
Cu(1)−N(4)	1.958(5)	1.954(5)	1.959(4)	1.959(4)
Cu(1)−O(3W)	2.748(6)	2.696(5)	2.749(7)	2.763(7)
Cu(1)−N(12)$^{\#2}$	2.868(6)	2.930(6)	2.864(6)	2.916(6)
M(1)−C(11)	1.908(5)	1.939(6)	1.945(5)	2.069(5)
M(1)−C(12)	1.908(6)	1.946(6)	1.952(5)	2.072(5)
M(1)−C(13)	1.903(7)	1.952(7)	1.947(6)	2.078(6)
N(11)−C(11)	1.139(7)	1.146(7)	1.145(6)	1.151(6)
N(12)−C(12)	1.142(7)	1.140(7)	1.142(7)	1.141(7)
N(13)−C(13)	1.142(7)	1.131(8)	1.136(7)	1.124(7)
Cu(1)---M(1)	5.267(1)	5.332(2)	5.287(1)	5.363(1)
Cu(1)---Ln(1)	5.616(2)	5.704(2)	5.622(2)	5.622(1)
M(1)---Ln(1)	5.564(1)	5.697(2)	5.596(2)	5.709(1)
O(1)−Ln(1)−N(11)	74.33(15)	74.35(15)	74.48(14)	74.37(14)
O(1)−Ln(1)−O(1W)	132.15(13)	129.32(13)	132.11(12)	131.71(12)
O(1)−Ln(1)−O(2)	68.14(13)	64.88(14)	68.07(12)	68.00(13)
O(2)−Ln(1)−N(11)	83.34(15)	83.88(15)	83.71(14)	83.91(14)
O(2)−Ln(1)−O(1W)	75.14(15)	74.92(15)	75.03(14)	75.19(14)
O(1W)−Ln(1)−N(11)	71.87(15)	71.60(14)	72.13(15)	71.60(15)
N(11)−Ln(1)−N(11)$^{\#1}$	143.4(2)	143.2(2)	143.3(2)	143.6(2)
C(11)−N(11)−Ln(1)	172.5(5)	171.0(5)	172.1(4)	173.0(4)
C(11)−N(11)−M(1)	178.2(5)	178.7(6)	179.2(5)	178.0(4)
N(12)−C(12)−M(1)	179.4(6)	178.3(6)	179.2(5)	178.0(5)
N(13)−C(13)−M(1)	178.1(5)	178.4(5)	178.2(5)	177.0(5)
N(12)$^{\#2}$−C(12)$^{\#2}$−Cu(1)	125.65(46)	123.95(50)	124.98(45)	122.57(46)

[a] Symmetry operations: #1, $-x, y, -z + 1/2$; #2, $-x + 1/2, -y + 3/2, -z + 1$.

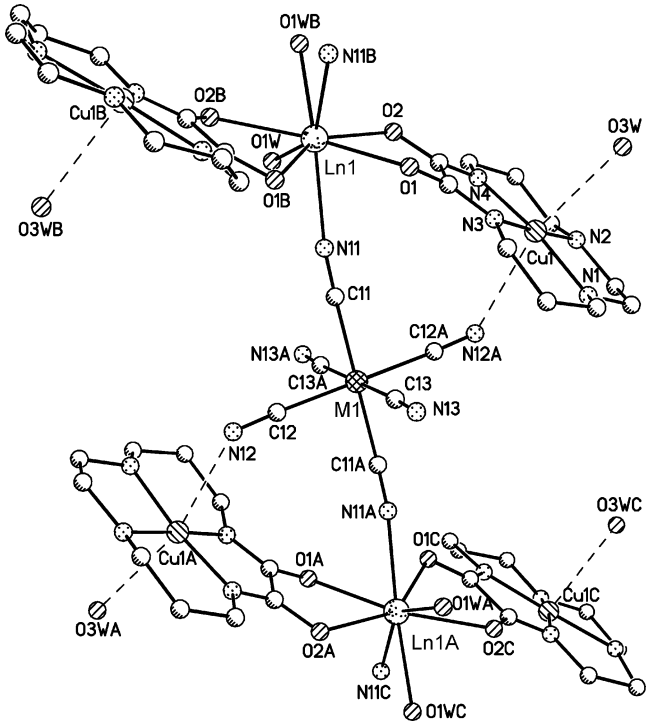

Figure 1. Structure of complexes **1**−**4**. Hydrogen atoms and the interstitial water molecules are omitted for clarity.

for **1**, 2.696(5) for **2**, 2.749(7) for **3**, and 2.763(7) Å for **4**. Therefore, the coordination environment of Cu(1) is a distorted octahedral with two long axial bonds. The four nitrogen atoms of L are situated at the equatorial plane with the Cu(1)−N bond distances ranging from 1.952(5) to 1.989(6) Å for **1**, from 1.947(5) to 1.984(6) Å for **2**, from 1.951(5) to 1.992(5) Å for **3**, and from 1.945(5) to 1.989(5) Å for **4**. The Cu(1)−N(amido) bond distances are shorter than that of the Cu(1)−N(amine) bonds, as has been observed in other oxamidato−Cu(II) complexes.[38,39,51] The adjacent metal−metal distances for M(1)---Gd(1) and M(1)---Cu(1) increase slightly in the order of Cr > Fe > Co, which is consistent with the increasing order of ionic radii. The Fe(1)---La(1) separation in **2** is larger than the Fe(1)---Gd(1) distance in **3**, which could be explained by the lanthanide contraction.

The hexacyanometalate(III) ion is approximately octahedral, and the M−C and C≡N bond distances and M−C≡N bond angles do not deviate greatly from the normal values.

The zigzag chains run parallel along the crystallographic *a* axis and are linked together through H-bonding between the uncoordinating cyano nitrogen atoms (N13) and the interstitial water molecules (O2W) giving rise to a 2D layer (*ab* plane), as shown in Figure 2a. The planes are further linked through H-bonds between O(3W) and O(2)$^{\#3}$ of different planes to yield a 3D network (Figure 2b). The intermolecular contacts are shown in Table 3.

Magnetic Properties. The temperature dependence of the $\chi_m T$ product/Cu_2GdCo unit for $[CuL]_2Gd(H_2O)_2Co(CN)_6 \cdot 7H_2O$ (**1**) is shown in Figure 3. The $\chi_m T$ value at room temperature is ca. 8.8 emu K mol^{-1}, close to the theoretical value of 8.625 emu K mol^{-1} ($g = 2.0$) with diamagnetic Co(III). The $\chi_m T$ value keeps nearly constant until 150 K, after which it increases smoothly until 7.4 K before it decreases rapidly. The magnetic susceptibility obeys the Curie−Weiss law with a positive Weiss constant $\Theta = +2.2$ K with the Curie constant $C = 8.72$ emu K mol^{-1}. This behavior is consistent with a Cu(II)−Gd(III) ferromagnetic interaction, upon which an intermolecular antiferromagnetic coupling is imposed. The possibility of the contribution of Cu(II)−Cu(II) antiferromagnetic exchange through Gd(III) was negligibly small due to the long Cu(II)---Cu(II) separation (10.80 Å).[49] On the basis of the structural information of **1**, the 1D chain can be regarded as Cu_2Gd trinuclear units connected by diamagnetic $[Co(CN)_6]^{3-}$. Therefore, the magnetic susceptibilities can be evaluated accordingly by the following expression derived from the Hamiltonian $\hat{H} = -2J_{GdCu}\hat{S}_{Gd}(\hat{S}_{Cu1} + \hat{S}_{Cu2})$:

$$\chi_m = \frac{Ng^2\beta^2}{6k(T-\Theta)} \frac{105 + 497e^{-16J/kT} + 252e^{-9J/kT} + 252e^{-7J/kT}}{6 + 10e^{-16J/kT} + 8e^{-9J/kT} + 8e^{-7J/kT}}$$

The best-fit parameters obtained are $J_{GdCu} = +2.2(1)$ cm^{-1}, $g = 1.99(1)$, and $\Theta = -0.49(2)$ K, among which Θ accounts for the intermolecular interaction. The agreement factor *R*, defined as $R = \Sigma(\chi_{obsd}T - \chi_{cald}T)^2/\Sigma(\chi_{obsd}T)^2$, is equal to 1.7×10^{-4}. It should be noted that the fit by including Cu^{II}−Cu^{II} coupling via Gd^{3+} gave similar values of J_{GdCu}, *g*, and Θ along with a J'_{CuCu} value with a large standard error, and therefore the value of J'_{CuCu} is set as zero during the fit. The intermolecular term should include the contribution of the

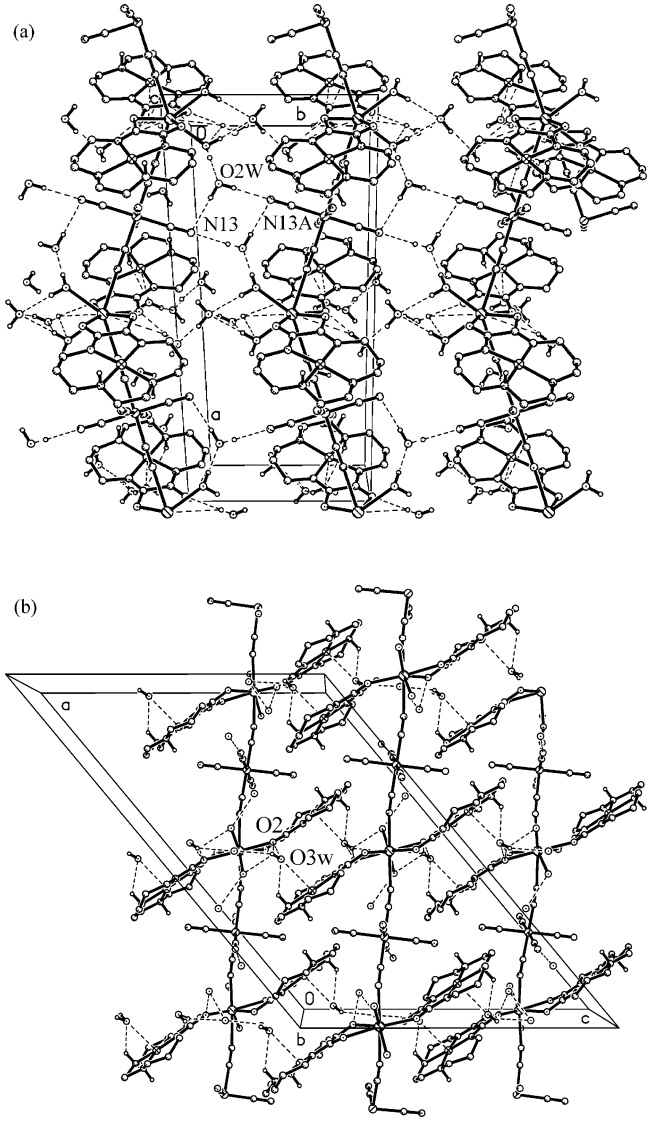

Figure 2. Interchain interactions: (a) along the *c* axis; (b) along the *b* axis.

Table 3. Intermolecular Contacts (Å)[a]

donor···acceptor	1	2	3	4
N2···O3W	3.188	3.250	3.184	3.133
N1···N12$^{\#2}$	3.175	3.241	3.159	3.148
O2W···N13	2.936	2.905	2.932	2.897
O1W···O5W	2.952	2.949	2.960	2.921
O4W···O1	2.779	2.800	2.785	2.770
O2W···N13$^{\#4}$	3.154	3.162	3.162	3.169
O5W···O4W$^{\#5}$	2.675	2.705	2.652	2.665
O1W···O2W$^{\#6}$	2.698	2.676	2.698	2.674
O1W···O3W$^{\#7}$	2.962	3.025	2.957	2.983
O3W···O5W$^{\#3}$	3.051	3.158	3.065	3.106
O3W···O2$^{\#3}$	2.845	2.821	2.849	2.839

[a] Symmetry operations: #1, $-x, y, -z + 1/2$; #2, $-x + 1/2, -y + 3/2, -z + 1$; #3, $-x, -y + 2, -z + 1$; #4, $-x + 1/2, -y + 1/2, -z + 1$; #5, $-x, y + 1, -z + 1/2$; #6, $x, y + 1, z$; #7, $x, -y + 2, z - 1/2$.

Cu(II)−Cu(II) coupling through the N≡C−Co−C≡N pathways. As discussed above, the positive exchange constant (J_{GdCu}) suggests the existence of Cu(II)−Gd(III) ferromagnetic interaction.

The field dependence of the magnetization (0−70 kOe) of **1** measured at 1.88 K shows saturation of the magnetization (inset of Figure 3), reaching the expected value of 9.0 $N\beta$ at 70 Oe for ferromagnetic Gd(III)−Cu(II) systems with $S_T = 7/2 + 2 \times 1/2 = 4.5$. The experimental data are higher than the corresponding values for uncoupling $S_{Gd} + 2S_{Cu}$ and are in good agreement with the Brillouin curve for an $S = 4.5$ spin state, which also confirms the $S = 4.5$ ground state for the complex.

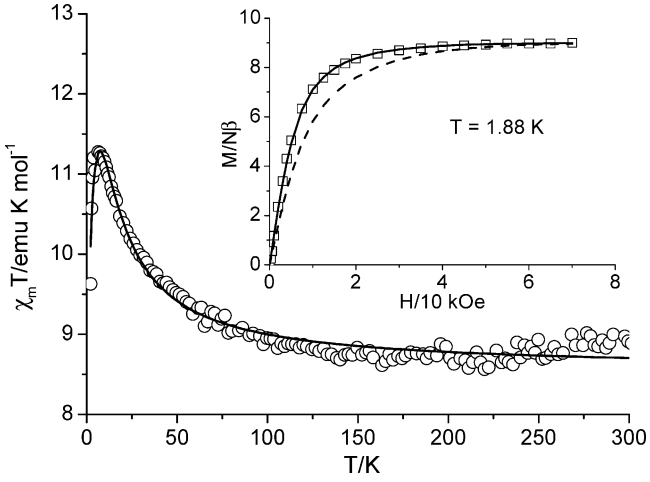

Figure 3. Plot of $\chi_M T$ vs temperature for **1**. The solid line represents the theoretical values based on the parameters described in the text. Inset: Field dependence of magnetization at 1.88 K for **1**. The solid lines represent the Brillouin function that corresponds to $S = 4.5$ (−) and noninteracting $S_{Gd} + 2S_{Cu}$ (−−) with $g = 2.0$.

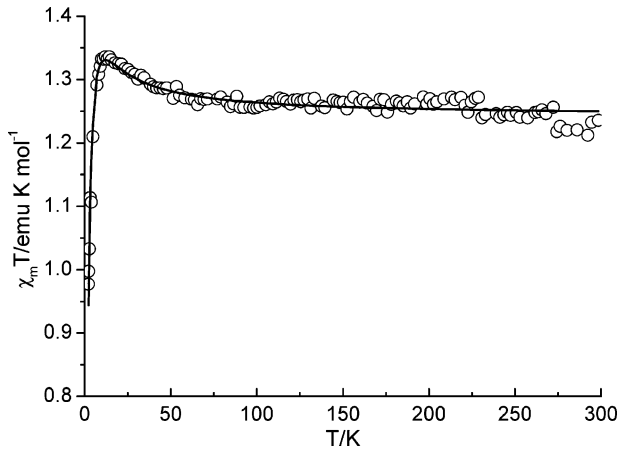

Figure 4. Plot of $\chi_M T$ vs temperature for **2**. The solid line represents the theoretical values based on the parameters described in the text.

The magnetic susceptibilities of $[CuL]_2La(H_2O)_2Fe(CN)_6 \cdot 7H_2O$ (**2**) have been measured under an applied field of 20 kOe in the temperature range 2−300 K. A plot of $\chi_m T$ vs. T for **2** is shown in Figure 4, where χ_m is the magnetic susceptibility per Cu_2LaFe unit. With the decrease of the temperature $\chi_m T$ increases slowly reaching a maximum value of 1.34 emu K mol^{-1} at 12 K and then decreases promptly, which indicates the presence of weak intramolecular ferromagnetic coupling on which a weak intermolecular antiferromagnetic interaction is imposed. The magnetic susceptibilities obey the Curie−Weiss law with a positive Weiss constant $\Theta = +0.98$ K and Curie constant $C = 1.25$ emu K mol^{-1}, which also proves the presence of an overall weak ferromagnetic behavior of the complex.

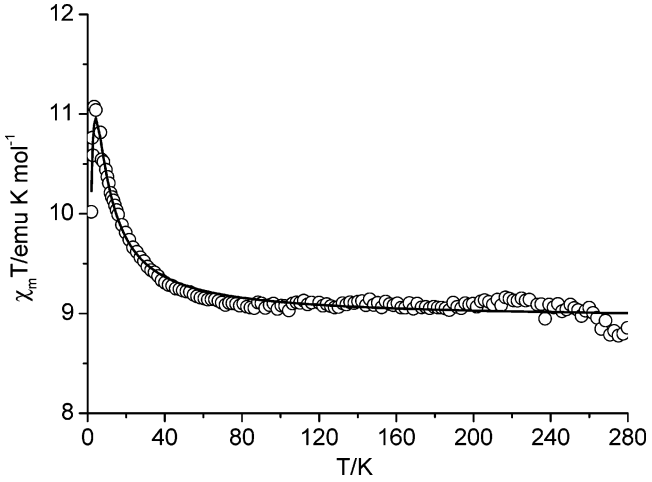

Figure 5. Plot of $\chi_M T$ vs temperature for **3**. The solid line represents the theoretical values based on the parameters described in the text.

Complex **2** provides an intriguing example to investigate the Fe(III)−Cu(II) magnetic interaction through the weak bridging cyano ligands. It is well-known that the magnetic exchange between Fe(III) and Cu(II) through cyano bridges is ferromagnetic. We may be interested in the strength of the $Fe^{III}-Cu^{II}$ coupling through such a weak bridging bond in complex **2** and in whether the nature of the magnetic coupling would change from ferromagnetic to antiferromagnetic. Considering that the Cu(II)−Cu(II) magnetic exchange through the diamagnetic La^{3+} ion is weak and usually antiferromagnetic, the magnetic behavior is mainly due to the Cu(II)−Fe(III) coupling. On the basis of the crystal data, the molecular chain can be expressed as cyano-bridged Cu_2Fe trimer connected by diamagnetic La^{3+} ions from the magnetic viewpoint. On the basis of this model, the magnetic susceptibilities of **2** have been approximated by the Hamiltonian $\hat{H} = -2J_{CuFe}\hat{S}_{Fe}(\hat{S}_{Cu1} + \hat{S}_{Cu2})$ giving the parameters $J_{CuFe} = +1.7(1)$ cm^{-1}, $g = 2.10(1)$, $zJ' = -0.70(1)$ cm^{-1}, and $R = 1.2 \times 10^{-4}$. This result indicates the ferromagnetic nature of the $Cu^{II}-Fe^{III}$ coupling through the weak cyano bridges.

Figure 5 shows the $\chi_m T$ vs T plot of $[CuL]_2Gd(H_2O)_2Fe(CN)_6 \cdot 7H_2O$ (**3**) measured in the temperature range of 2−280 K under 5 kOe. The increase of $\chi_m T$ with a decrease of temperature suggests the presence of global ferromagnetic interactions between adjacent metal ions. The Weiss constant derived from the χ_m^{-1} vs T plot is equal to +1.0 K with the Curie constant of 9.03 emu K mol^{-1}, which is consistent with the calculated value of 9.0 emu K mol^{-1} ($g = 2.0$) per Cu_2GdFe.

Crystal data for **3** show the presence of ligand-bridged $Cu^{II}-Gd^{III}$ and $Gd^{III}-Fe^{III}$ ions. The 1D chain can be regarded as an alternating Cu_2Gd trimer and $[Fe(CN)_6]^{3-}$ (model 1) or, alternatively, as a GdFe chain and two [CuL] groups (model 2). To estimate the intermetallic coupling constants, we assumed that the magnetic exchanges between the trimer and $[Fe(CN)_6]^{3-}$ in model 1 and between the GdFe chain and [CuL] in model 2 are negligibly small. These are rough models and should be carefully used. The premise is that the intratrimer coupling is much stronger than the Fe(III)−trimer interaction.

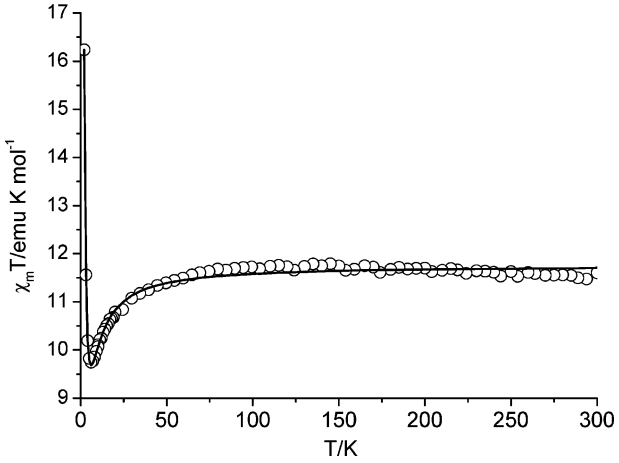

Figure 6. Plot of $\chi_M T$ vs temperature for **4**. The solid line represents the theoretical values based on the parameters described in the text.

Equation 1 derived from model 1 contains g, J_{GdCu}, and Θ that account for the intermolecular interaction and weaker magnetic exchange between Fe(III) and the Cu_2Gd trimer. The fitting gave the parameters of $J_{CuGd} = +0.98(5)$ cm^{-1}, $g = 1.99(1)$, $\Theta = -0.48(1)$ K, and $R = 9.0 \times 10^{-5}$. The positive $Cu^{II}-Gd^{III}$ exchange coupling parameter shows the ferromagnetic nature, while the negative Θ value suggests that the ferromagnetic Cu(II)−Fe(III) interaction is overwhelmed by the antiferromagnetic[16,57] $Gd^{III}-Fe^{III}$ and intermolecular coupling. Besides, it should be noted that the employment of an identical g value for the fitting is unreasonable; however, such a simplification does not affect significantly the fitting results.

$$\chi_M = \frac{(\chi_{trimer} + \chi_{Fe})T}{T - \Theta}$$

$$\chi_{Fe} = \frac{Ng^2\beta^2}{3kT} S_{Fe}(S_{Fe} + 1) \qquad (1)$$

When model 2 was used for the fitting, eq 2 can be employed. The χ_{chain} (per GdFe) expression has been derived by using the tetranuclear Gd_2Fe_2 square ($H = -2J_{GdFe}(S_{Gd(1)}S_{Fe(2)} - S_{Gd(1)}S_{Fe(4)} - S_{Gd(3)}S_{Fe(2)} - S_{Gd(3)}S_{Fe(4)})$) to simulate an alternating GdFe chain on the condition that J_{GdFe} is small (see Supporting Information).[58,60] However, no satisfactory fitting parameters could be obtained, which indicates that model 2 is inappropriate.

$$\chi_M = \frac{(\chi_{chain} + 2\chi_{Cu})T}{T - \Theta}$$

$$\chi_{Cu} = \frac{Ng^2\beta^2}{3kT} S_{Cu}(S_{Cu} + 1) \qquad (2)$$

The magnetic properties of $[CuL]_2Gd(H_2O)_2Cr(CN)_6 \cdot 7H_2O$ (**4**) are different from that of the CuGdFe analogue (**3**). Figure 6 shows the magnetic susceptibilities of **4** in the form of $\chi_m T$ vs T per Cu_2GdCr unit. The $\chi_m T$ value decreases gradually down to ca. 6 K and then increases sharply reaching a value of 16.2 emu K mol^{-1} at 2 K. The magnetic susceptibility obeys the Curie−Weiss law with a negative Weiss constant Θ of −0.64 K and the Curie constant of 11.6

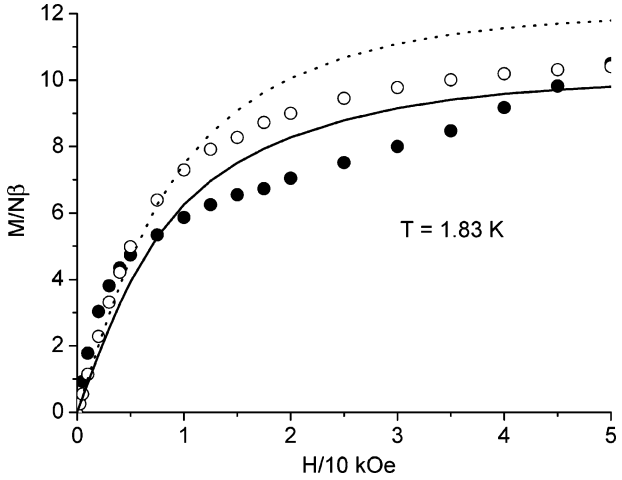

Figure 7. Field dependence of magnetization for **3** (○) and **4** (●). The lines represent the Brillouin function that corresponds to noninteracting $2S_{Cu} + S_{Fe} + S_{Gd}$ (solid) and $2S_{Cu} + S_{Cr} + S_{Gd}$ (dotted) with $g = 2.0$.

emu K mol^{-1}, which is similar to the calculated value of 10.5 emu K mol^{-1} ($g = 2.0$). These data clearly show the existence of overall antiferromagnetic interactions in the complex.

Using the approximate approaches similar to those for complex **3**, we tried to estimate the magnitude of the intermetallic magnetic exchange. The expressions based on model 1 gave bad fitting results, which suggests that model 1 is not suitable.

The best fit to the experimental data by using model 2 gives the parameters $J_{GdCr} = -0.35(1)$ cm^{-1}, $g = 2.12(1)$, $\Theta = +1.21(1)$ K, and $R = 8.9 \times 10^{-5}$. The negative Cr(III)−Gd(III) coupling constant is typical of an antiferromagnetic interaction, which is in good agreement with that of other cyano-bridged Cr(III)−Gd(III) compounds.[58−61] The positive Θ value includes the contribution of Cu(II)−Gd(III) coupling, which shows the presence of a ferromagnetic Cu^{II}−Gd^{III} interaction. This result is reasonable, since the isostructural Cu_2Gd trimeric units in complexes **1**, **3**, and **4** should exhibit ferromagnetic Cu(II)−Gd(III) exchange with one accord.

Undoubtedly, the experimental curve of complex **4** is different from that of the analogous complex **3**. This may be due to the fact that the antiferromagnetic Gd(III)−M(III) coupling is different in strength: stronger in complex **4** than in complex **3**. Strong antiferromagnetic Gd(III)−Cr(III) coupling in **4** (even stronger than the Cu(II)−Gd(III) magnetic coupling) gives rise to an overall antiferromagnetic behavior. For complex **3**, weak antiferromagnetic Gd(III)−Fe(III) interaction is overwhelmed by the comparatively strong ferromagnetic Gd(III)−Cu(II) interaction generating global ferromagnetic properties. The models used for the fit are also consistent with the above suppositions.

The field dependences of the magnetization at 1.83 K for complexes **3** and **4** show marked differences between two complexes (Figure 7). For complex **3**, the magnetization saturates rapidly reaching 10.4 $N\beta$ at 50 kOe. The experimental curve lies above the theoretical curve for uncoupled two Cu^{2+} ($S = 1/2$), one Gd^{3+} ($S = 7/2$), and one Fe^{3+} ($S = 1/2$) spins, indicating the global ferromagnetic interaction in the complex. The magnetization of **4** shows a regular increase at low fields and reaches a plateau of ca. 8 $N\beta$ before increasing linearly again. This behavior indicates the presence of antiferromagnetic intermetallic coupling similar to the previously reported $Cr^{III}Gd^{III}$ complexes.[60] This phenomenon reveals that the antiferromagnetic Cr(III)−Gd(III) magnetic interaction is dominant in complex **4**.

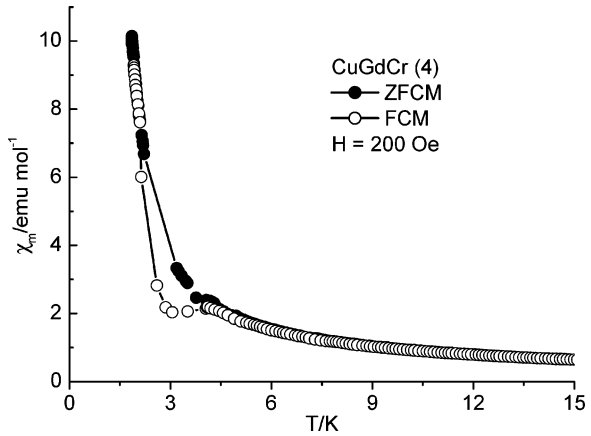

Figure 8. Field-cooled magnetization (FCM) and zero-field-cooled magnetization (ZFCM) for **4**.

Scheme 1. Spin Frustration in the Three-Spin Compound (**4**)

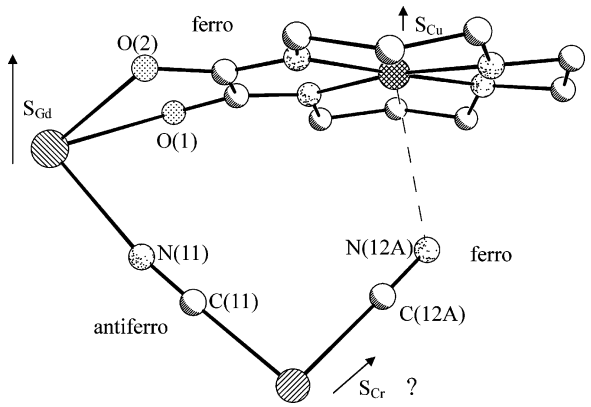

Another feature for the three-spin compounds is that spin frustration may exist in the cyclic Cu^{II}−Gd^{III}−M^{III} (M = Fe (**3**), Cr (**4**)) units if the couplings of J_{CuGd}, J_{CuM}, and J_{GdM} are of competing magnitude (Scheme 1). The FCM and ZFCM measurements of complex **4** showing divergence at 4.0 K support such a possibility (Figure 8).

The magnetic studies of complexes **3** and **4** indicate that the three-spin compounds[62] are not good candidates for quantitative magnetic investigation. Nevertheless, the three-spin magnetic materials with both antiferromagnetic and ferromagnetic interactions might exhibit interesting magnetic phenomena, for example spin frustration.

Similar to that of complex **2**, the magnetic properties of $[CuL]_2La(H_2O)_2Cr(CN)_6 \cdot 7H_2O$ (**5**) (Figure 9) indicate the

(61) Sanada, T.; Suzuki, T.; Yoshida, T.; Kaizaki S. *Inorg. Chem.* **1996**, *37*, 4712.

(62) Madalan, A. M.; Roesky, H. W.; Andruh, M.; Noltemeyer, M.; Stanica, N. *Chem. Commun.* **2002**, 1638. Verani, C. N.; Weyhermüller, T.; Rentschler, E.; Bill, E.; Chaudhuri, P. *Chem. Commun.* **1998**, 2475. Vostrikova, K. E.; Luneau, D.; Wernsdorfer, W.; Rey, P.; Verdaguer, M. *J. Am. Chem. Soc.* **2000**, *122*, 718.

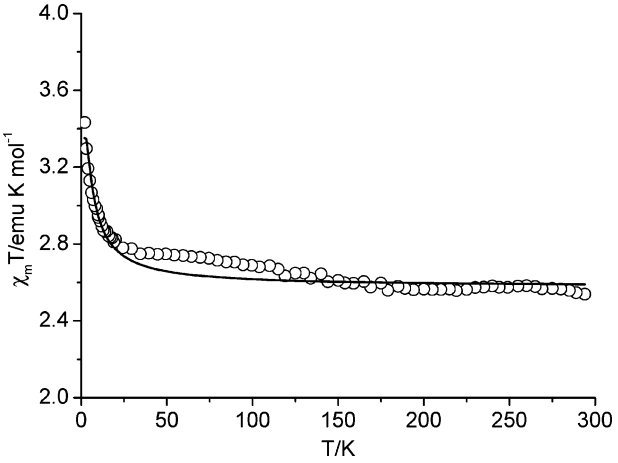

Figure 9. Plot of $\chi_M T$ vs temperature for **5**. The solid line represents the theoretical values based on the parameters described in the text.

existence of overall ferromagnetic coupling. The data obey the Curie−Weiss law with the Weiss constant of $\Theta = +1.13$ K and the Curie constant of $C = 2.65$ emu K mol^{-1}. The positive Weiss constant indicates a ferromagnetic interaction between Cu(II) and Cr(III). The magnetic susceptibilities can be fitted by the spin-Hamiltonian (eq 3) on the basis of a symmetrical linear Cu_2Cr trinuclear structure including an intermolecular interaction term.

$$\hat{H} = -2J\hat{S}_{Cr}(\hat{S}_{Cu1} + \hat{S}_{Cu2}) \quad (3)$$

The expression (eq 4) derived from the above Hamiltonian reproduce the experimental data satisfactorily giving the parameters of $J = +0.50$ cm^{-1}, $g = 1.98$, and $\Theta = -0.43$ K. The fitting results clearly show the presence of weak ferromagnetic coupling between Cu(II) and Cr(III) through the weak bridging pathways. The weak intermolecular antiferromagnetic exchange (Θ) is most probably transferred via the diamagnetic La^{3+} ions.

$$\chi_m = \frac{Ng^2\beta^2}{4k(T-\Theta)} \cdot \frac{10 + e^{-5J/kT} + 10e^{-2J/kT} + 35e^{3J/kT}}{2 + e^{-5J/kT} + 2e^{-2J/kT} + 3e^{3J/kT}} \quad (4)$$

Temperature dependence of field-cooled magnetization and zero-static ac magnetic susceptibilities of **3** and **4** show the absence of magnetic ordering until 1.8 K (see Supporting Information). The search for lanthanide-bearing molecule-based magnets remains a challenge.[63]

Conclusions

The present research provides a way of synthesizing mixed ligand-bridged heterotrimetallic 4f−3d coordination polymers. Five new 1D complexes have been prepared and found to possess interesting molecular structure and magnetic properties. The weak bridging cyanide ligands have been found to still transfer ferromagnetic interaction between Cu(II) and Cr(III)/Fe(III) ions, as do the strong bridging CN^- ligands. As usual, the oxamidato-bridged Cu(II)−Gd(III) ions interact ferromagnetically. Due to the low dimensionality of the species, no magnetic phase transition is observed; however, a spin frustration has been observed in the three-spin compound (**4**) as a result of the presence of ferro−ferro−antiferromagnetic exchanges in the trigonal Cu−Gd−Cr units. Future work will involve the synthesis of NiL-containing analogues for the elucidation of the magnetic coupling through cyanide bridges and the interaction between 3d metal ions and anisotropic 4f ions.

Acknowledgment. This work was supported by the National Natural Science Foundation of China (Project Nos. 20201008 and 50272034). K.H.-Z. thanks Prof. Yadong Li for helpful discussions and for providing excellent working conditions. We are also grateful to Prof. Song Gao for the magnetic measurements.

Supporting Information Available: Powder XRD patterns of complexes **5**, **2** (calculated), and **4** (calculated), a TGA curve of **2**, plots of zero-static ac magnetic susceptibilities for **3** and **4**, and an X-ray crystallographic file in CIF format. This material is available free of charge via the Internet at http://pubs.acs.org.

IC0348502

(63) Zhao, H.; Bazile, M. J., Jr.; Galan-Mascaros, J. R.; Dunbar, K. R. *Angew. Chem., Int. Ed.* **2003**, *42*, 1015.